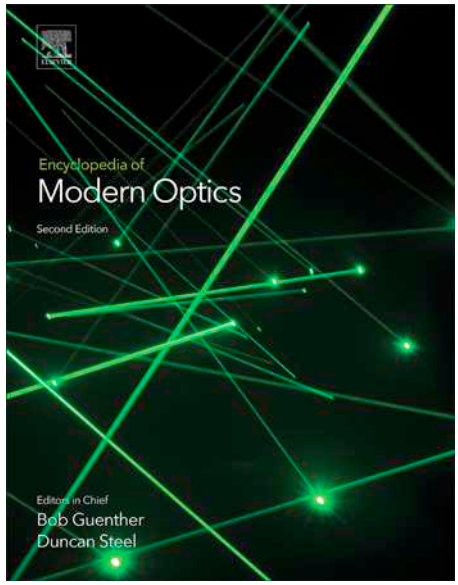




Benjamin S. Williams, Qing Hu (2018) Terahertz Lasers. In: Guenther, R. and Steel, D. (eds.), Encyclopedia of Modern Optics 2nd edition, vol. 1, pp. 379–386. Oxford: Elsevier.

# Terahertz Lasers

**Benjamin S Williams,** University of California, Los Angeles, CA, United States
**Qing Hu,** MIT, Cambridge, MA, United States



## Optically Pumped Molecular Gas Lasers

The first commercially available terahertz lasers (more traditionally known as far-infrared or sub-millimeter wave lasers) were gas lasers, where stimulated emission takes place between rotational levels of excited vibrational states of low-pressure molecular gasses. The first such demonstration was made in 1963, where lasing in water vapor excited with a pulsed electric discharge was observed by Crocker *et al.* (1964). Gas lasers continue to be an important THz laser source, although now the most common arrangement is to use optical pumping by a $CO_2$ gas laser (Chang and Bridges, 1970), which significantly increases the pumping selectivity and efficiency (**Fig. 1**). A large variety of discrete lines can be obtained between 0.1 and 8 THz (Inguscio *et al.*, 1986), although most strongly pumped lines are below 3 THz. Continuous-wave power levels of milliwatts are not uncommon, with powers of hundreds of milliwatts possible for the strongest lines (e.g. the methanol lines at 118.8 and 184.3 μm). There have been many review articles published on far-IR gas lasers, including (Jacobsson (1989), Inguscio *et al.* (1986), Dodel (1999)), and they are commercially available from several vendors.

The selection of laser frequencies is limited by available gasses, some of which are "inconvenient" to handle from a safety and environmental point of view. Only discrete tuning of the lasers is available because of the limited transition lines, however harmonic generators can be used to generate tunable sidebands (Farhoomand *et al.*, 1985). Although these laser systems present limitations in terms of size and weight, this has not prevented them from being flown into space. For example, a far-IR gas laser was used as a 2.5 THz local oscillator source in the Earth Observing System (EOS) Aura satellite, in the Microwave Limb Sounder heterodyne instrument. This laser delivered ~30 mW of cw power while consuming 120 W of electrical power (Mueller *et al.*, 2007).

It is notable that THz molecular gas lasers can operate at room temperature, even though the THz photon energy ($h(\nu) \sim 1$–$30$ meV) is smaller than the thermal energy $k_BT$. This is in contrast to the THz semiconductor lasers to be discussed below, all of which require varying degrees of cryogenic cooling. A naïve assumption is sometimes made that a population

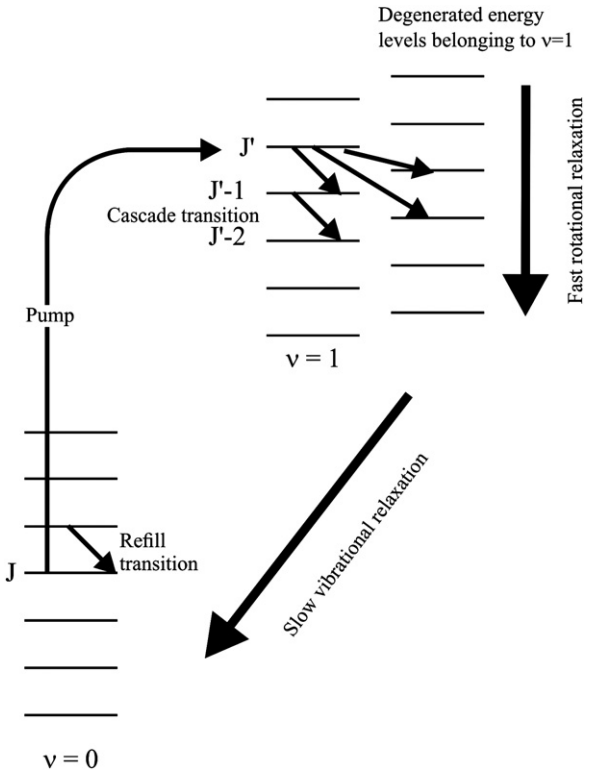


**Fig. 1** Schematic of energy levels and transitions in a generic far-IR molecular gas laser. The pump photon excites the selected molecule from its vibration ground state to an excited vibrational state. FIR laser action takes place between rotational levels in the excited state. Figure from Jacobsson, S., 1989. Optically pumped far infrared lasers. Infrared Phys. 29, 853–874.

inversion is not possible if ($h(v) < k_B T$). However, one must remember that a pumped laser system is by its nature not in thermal equilibrium. A population inversion is possible as long as the lower state lifetime is shorter than the upper to lower state relaxation time ($\tau_1 < \tau_{21}$). Rotational transitions in a low-pressure gas have very little broadening ($\sim$1–20 MHz), due to the weak scattering processes (Jacobsson, 1989). As a result, the energy states are very distinct, and can maintain different relaxation rates. Second, the narrow linewidths lead to large cross sections, and high peak levels of gain even for modest population inversion levels.

The inherent limitations of the molecular gas lasers (i.e. size, weight, limited tunability, and low power efficiencies etc.) have created interest in developing terahertz semiconductor lasers. One need look no further than the success of the interband diode lasers in the visible and near-infrared wavelengths, to see the inspiration for developing (potentially) low cost, compact, coherent sources. However, the terahertz photon energies are 100–1000 times smaller than visible photons - appropriate materials that have both a small bandgap and can support a population inversion simply do not exist in nature. As a result, semiconductor terahertz laser research has focused on unconventional sources of stimulated emission. We will highlight three of these here: the germanium intra-valence band lasers, silicon impurity-state lasers, and quantum-cascade lasers.

## Germanium Intra-Valence Band Lasers

The first type of THz semiconductor laser demonstrated was the hot-hole p-Ge laser. In this device, lasing action results from a hole population inversion in bulk p-Ge that is established between the light and heavy hole bands due to a "streaming motion" that takes place in crossed electric and magnetic fields (Golka *et al.*, 1991). For low lattice temperatures ($<$20 K), holes have kinetic energies far below the optical phonon energy (37 meV), and their energy relaxation is mediated by (relatively) slow acoustic phonons and impurity scatterings. However, for critical ratios of the electric to magnetic field strength, heavy holes are less bent by the magnetic field due to their heavier mass and therefore can acquire more energy from the electric field and be accelerated to have sufficient kinetic energy to emit an optical phonon, and quickly relax to lower energies. Light holes acquire insufficient energy and do not scatter by the optical phonon. This acts as a pumping mechanism which establishes a population inversion between the light hole and heavy hole bands (**Fig. 2**).

Large fields are required: typical electric fields strengths are from 1 to 2 kV/cm and magnetic fields greater than 1 T. Hence, a liquid-helium cooled superconducting magnet is typically used. The gain is relatively low, as the pumping mechanism is highly nonselective and inefficient, and the upper state lifetime is still relatively short. Free-carrier absorption is also an issue, and the doping must be kept low ($<10^{15}$ cm$^{-3}$). Nonetheless, due to the large total semiconductor volume, large peak powers of several Watts have been obtained in pulsed mode. Absent a cavity mode selection mechanism, broadband lasing is obtained (spanning over 10–20 cm$^{-1}$) that can be tuned from 1–4 THz by the applied electric/magnetic fields. Its broadband gain has proven useful for mode-locked operation, where pulses with a 100-ps width have been obtained (Hovenier *et al.*, 2000). However the need for a strong magnetic field, high voltage, and cryogenic operation (T$<$20 K) has limited the utility of this source. Traditionally, due to high power consumption and low efficiency the maximum duty cycle is usually limited to less than $10^{-4}$, although a report of up to 5% duty cycle has been demonstrated (Bründermann *et al.*, 2000).

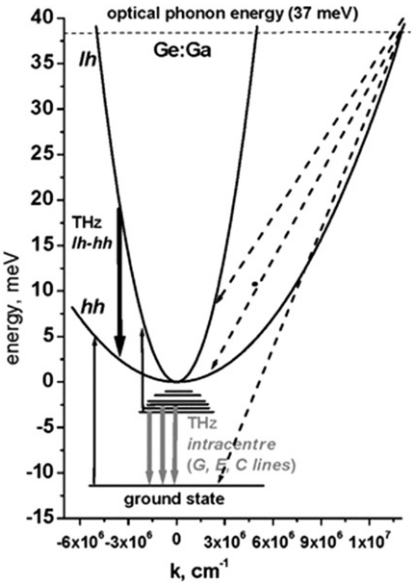


**Fig. 2** Schematic of intra-valence band transitions in p-Ge lasers with the hole energies plotted in positive direction. Dashed arrows correspond to relaxation of holes due to interaction with optical phonons; the bold black downward arrow indicates stimulated emission from light- to heavy-hole subband. Figure from Hübers, H.-W., Pavlov, S.G., Shastin, V.N., 2005. Terahertz lasers based on germanium and silicon. Semicond. Sci. Technol. 20, S211–S221.

A related device is the strained p-Ge resonant state laser. *cw* lasing that was tunable with pressure from 2.5 to 10 THz was demonstrated (Gousev *et al.*, 1999). Power levels of tens of microwatts were observed and operation takes place at liquid helium temperatures. In this device, application of strain lifts the degeneracy of the light-hole and heavy-hole band such that the 1 s impurity state of the heavy-hole band is brought into resonance with the light-hole band. This leads to a population inversion between the heavy hole 1 s state and the light-hole impurity states, which are depopulated by electric field ionization. No magnetic field is necessary. A similar laser was demonstrated in 2000 in SiGe/Si quantum wells, where the mechanism of lasing is the same but the strain is provided instead by the epitaxial mismatch (Kagan *et al.*, 2000; Blom *et al.*, 2001). This is a promising method which eliminates the need for externally applied strain, but the power level is still quite low and high voltage (300–1500 V) is required.

## Silicon Impurity State Lasers

Silicon is not ordinarily considered a promising material for semiconductor lasers, due to its indirect bandgap. However, *n*-type silicon crystals can be used to make optically pumped 4-level terahertz lasers, based upon donor intracenter radiative transitions. Reviews are given in Hübers *et al,*. (2005), Pavlov *et al.* (2013). Silicon is an attractive material for THz applications in general; unlike III-V semiconductors it is non-polar and has low lattice absorption in the THz range. Various donor impurities have been demonstrated for lasing, including As, P, Sb, and Bi. Excepting a few outliers, lasing has mostly been observed between 1–2 THz and 5–7 THz as shown in **Fig. 3**. Population inversion is obtained between states based upon varying rates of electron relaxation mediated by acoustic and optical phonons. Cavities are formed by polishing bulk crystals with sizes of several millimeters on a side. If desired, stress can be applied to modify the lasing frequency or improve the performance.

A schematic of the energy states and relaxation pathways is shown in **Fig. 3** for several different donor species. Typical donor densities are in the range of $10^{15}$–$10^{16}$ cm$^{-3}$. Pumping occurs via photoionization of the impurity ground state into the conduction band, typically performed using a mid-infrared $CO_2$ laser. After the electron is excited high into the conduction band, it relaxes via emission of optical and acoustic phonons until it is captured in the high-excited donor states, whereupon it relaxes via emission of acoustic phonons along specific paths that depend upon the energy structure of the particular donor. For example, in Si:Sb and Si:P this relaxation ends in a long lived state ($2p_0$) with an estimated lifetime of hundreds of picoseconds. Lasing occurs between the $2p_0 \rightarrow 1s$ ($T_2$), where the lower radiative state is estimated to have a lifetime of 10–100ps.

Typical pump threshold intensities are in the range of 10–300 kW/cm$^2$, depending upon the donor type, concentration, and stress. Peak powers on the order of milliwatts have been measured. In order to avoid thermal ionization of the impurities, and thermal backfilling of the lower radiative state, operation requires cryogenic temperatures typically $<10$ K, although operation up to 30 K has been observed for Si:Bi lasers. Furthermore, decay dynamics of the nonequilibrium phonon distribution limits the laser operation to pulsed mode – for example in Si:P and Si:Sb lasers emission is quenched after $\sim$150 ns. The operating temperature may be potentially improved by the use of impurities with deeper energy states, so as to increase the energy barrier for thermal backfilling. Research is ongoing to better understand the complexities of the relaxation physics, as well as to improve the performance.

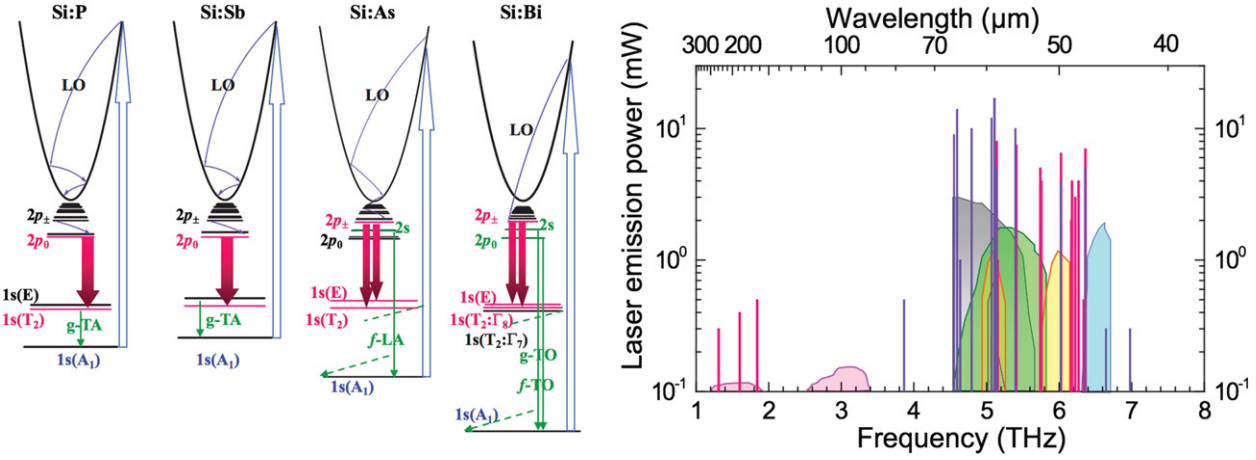


**Fig. 3** (left) Laser schemes realized in Si: P, Si: Sb, Si:As and Si:Bi when pumped with a $CO_2$ laser into the conduction band. The straight blue arrows up indicate the optical pumping and the bold red arrows down are for stimulated emission. Resonant coupling with intervalley phonons is shown by green vertical arrows down. (right) Various reported laser lines from various optically pumped Si impurity state lasers. Figures from Pavlov, S.G., Zhukavin, R.K., Shastin, V.N., H.-W., 2013. The physical principles of terahertz silicon lasers based on intracenter transitions. Phys. Status Solidi B250, 9–36.

## Quantum-Cascade Lasers

At present, the most active area in THz laser research is in the field of terahertz quantum-cascade (QC) lasers. The QC-laser is a unipolar intraband laser in which photons are generated as electrons within the conduction band make radiative transitions between quantized subbands engineered into heterostructure quantum wells. By designing sophisticated sequences of coupled quantum wells, "one dimensional artificial molecules" are created with energy levels of the subbands designed to emit photons in the mid-infrared or terahertz spectral range. Furthermore, it is possible to achieve a fine degree of control over electron transport, such that electrons can be injected (usually) via resonant tunneling into an upper radiative state, and can be selectively depopulated from the lower state with some combination of tunneling and scattering processes. The radiative cross-section of the radiative transition can likewise be engineered by controlling the overlap and parity of the various wavefunctions.

The first THz quantum-cascade lasers were demonstrated in 2001 and shortly thereafter (Köhler *et al.*, 2002; Rochat *et al.*, 2002; Williams *et al.*, 2003); their technological progress has been summarized in various review articles (Williams, 2007; Kumar, 2011; Vitiello *et al.*, 2015). The most common material system is GaAs/$Al_xGa_{1-x}$ As heterostructures grown by molecular beam epitaxy, although other material systems have been demonstrated as well (e.g. InGaAs/AlInAs, InGaAs/GaAsSb, etc.). A common feature of these polar III-V semiconductors, is that they all exhibit strong electron interaction with longitudinal optical (LO) phonons (which typically have energies from 30–50 meV). At this time various THz QC-lasers currently have been demonstrated between 1.2 and 5.6 THz (and at frequencies as low as 0.6 THz in a very strong magnetic field).

So far cryogenic operation is still required for THz QC-lasers; the current temperature record is $T_{max}=200$ K in pulsed mode (<1% duty cycles), and $T_{max}=129$ K in cw mode without the assistance of a magnetic field. By applying a strong magnetic field perpendicular to the planes of quantum wells, additional quantization can be achieved in the transverse dimensions, which reduces the available scattering volume in the momentum space and consequently increases the upper-state lifetimes. As a result, a significant increase of the maximum operating temperature is achieved, from 165 K to 225 K, and the latter is still the record of all the solid-state THz lasers at this writing (Wade *et al.*, 2009). While efforts to improve temperature performance of the active material continue, with ongoing improvements in cryogen-free coolers, and considering the modest power consumption requirements, even operation in the 40–90 K range is very feasible for many applications. For devices operating above 77 K in cw, milliwatt level powers are typical, although in some cases very high powers have been observed. Current record results stand at over 2 W peak power in pulsed mode, and 230 mW in continuous-wave (cw) mode for devices cooled by liquid helium. Furthermore, wall-plug power efficiencies (WPE) greater than 1% have been achieved by several groups.

## Active Regions

The heart of the quantum-cascade laser is the multiple-quantum-well active region. Most active region designs can be grouped into three categories: bound-to-continuum (BTC), resonant-phonon (RP) designs, as well as hybrid designs which combine features of each. Schematics for the bandstructure and energy levels are shown in **Fig. 4**.

The key to the BTC design is the coupling of several quantum wells together to create a superlattice which supports a "miniband" of subband states when the appropriate electric field is applied. The radiative transition takes place between an isolated upper "bound" state that resides above the miniband, and a lower state which is the top state of the miniband. Generally speaking, intra-miniband scattering is favored over scattering out of the bound state, which creates a population inversion at lower temperatures. Owing to the relatively small widths of the minibands (about 15–20 meV) for THz QCLs, LO-phonons are not directly involved in the depopulation process. Since the energy drop per module is relatively small, and the oscillator strength is large, this design is often characterized by low threshold voltages and currents, although performance tends to drop off rapidly with rising temperature above 100 K.

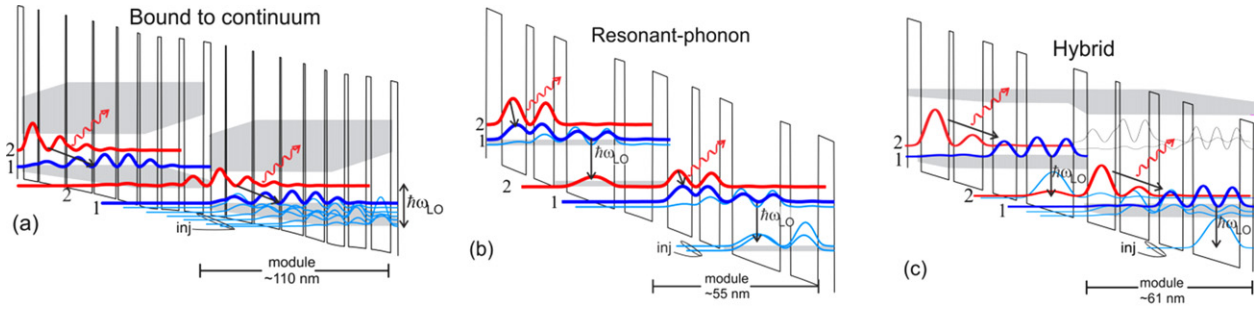


**Fig. 4** Schematic figure of the conduction band edge (Gaas/$Al_xGa_{1-x}$As heterostructures) and energy levels of three types of active regions for quantum-cascade lasers. Two repeated modules are shown in each case. Energy levels are plotted with the probability density of the bound-state. Radiative transition occurs between levels 2 and 1. Also shown for (b) and (c) are electron relaxation via emission of longitudinal optical phonons. Figure adapted from Williams, B.S., 2007. Terahertz quantum cascade lasers. Nat. Photon. 1, 517–524.

The other major active region type is the resonant phonon (RP) scheme. This design, a reservoir/injector state is designed to reside 36 meV (one LO phonon energy) below the lower radiative state. This encourages fast depopulation via electron-LO-phonon scattering into the reservoir state. In order to prevent simultaneous depopulation of the upper state, the energy levels are designed so that electrons are selectively removed via resonant tunneling from the lower state only. In general, RP and hybrid designs have better temperature performance than the BTC designs. Good RP/hybrid designs regularly operate above 130 K and even as high as 200 K in pulsed mode. The explicit inclusion of an LO-phonon scattering event for depopulation results in a more robust depopulation mechanism, as well as a larger energetic barrier to thermal backfilling of electrons from the reservoir.

Several issues are limiting further improvements of the temperature performance of THz QC-lasers so far. Unlike gas lasers, electrons within QC-lasers exist within a high density solid-state matrix: they interact strongly with the lattice, other carriers, and have a large density of states available for scattering. As a result, lifetimes are picoseconds or shorter, and the energy level broadenings are on the order of hundreds of GHz or larger. This not only reduces the peak gain cross-section, but also tends to blur energy levels, making it difficult to maintain selective injection and depopulation essential to achieve a population inversion. This problem is exacerbated for THz QC-lasers at lower frequencies ($<2$ THz), as the energy spacing becomes comparable with the level broadening.

The second major issue is thermally activated scattering and leakage that degrade the upper state lifetime for high electron temperatures. For example, as electrons in the upper subband acquire sufficient in-plane kinetic energy, they may emit an LO-phonon and relax to the lower subband, or tunnel into the continuum. There is active research underway to suppress these mechanisms, which primarily involves the development of novel active region designs. In addition, new heterostructure material systems are also under investigation. For example, GaN-based materials are attractive since GaN has a much larger LO-phonon energy (90 meV) compared to most III-Vs, which should in principle suppress thermally activated LO-phonon scattering. An even more radical approach is to develop quantum-dot based cascade lasers: the discrete density of states is predicted to suppress nonradiative and dephasing scattering to improve high temperature operation. Nonetheless, no lasers have been reported to date using these new material/structure approaches.

## Waveguides and Cavities

The biggest difference between THz QC-lasers and semiconductor lasers at shorter wavelengths lies in the techniques for waveguiding. Conventional dielectric waveguides (as used for semiconductor diode lasers and mid-IR QCLs) are impractical for THz QC-lasers. Due to the $\lambda 2$ scaling of free-carrier loss, the use of doped cladding layers introduces excessive loss at THz wavelengths. Hence, two types of unique waveguides for THz QC-lasers have been developed that minimize the overlap of the mode with doped semiconductor, and instead use metal layers partially or fully for optical confinement; unlike at shorter wavelengths losses are quite modest for noble metals in the terahertz range. These two schemes are shown in Fig. 5.

The first type is the surface-plasmon (SP) waveguide, which involves the growth of a thin (0.2–0.8 μm thick) heavily doped layer underneath the 10 μm-thick GaAs/AlGaAs quantum-well active region, but on top of a semi-insulating GaAs substrate. The resulting mode is a compound surface plasmon tightly confined by the top metal contact, and loosely bound to the heavily doped lower plasma layer. The mode extends far into the substrate (by tens to hundreds of microns); since the substrate is semi-insulating, the free carrier loss is minimal. The downside is that ridges narrower than $\sim 100$ μm tend to squeeze the mode out of the active region and into the substrate, which effectively puts a floor on the minimum device area (and power dissipation), which in turn limits the maximum achievable cw operating temperature.

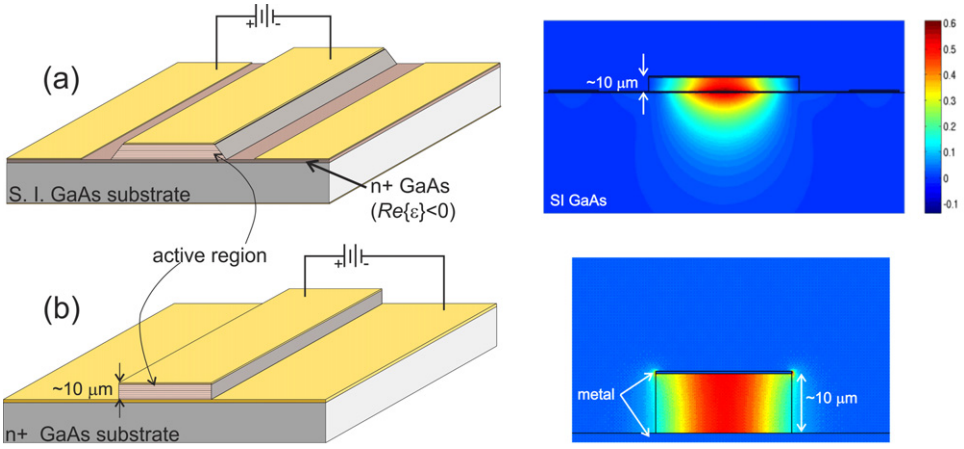


**Fig. 5** Schematic of terahertz QC-laser waveguides. Schematic diagram (left) and typical two-dimensional mode intensity pattern (right) for (a) surface plasmon waveguides and (b) metal-metal waveguides. Re($\varepsilon$) $<0$ indicates that the real part of the permittivity is less than zero in the heavily doped GaAs laser. Figure from Williams, B.S. 2007. Terahertz quantum cascade lasers. Nat. Photon. 1, 517-524.

An alternative to the SP waveguide is the so-called "metal-metal" (MM) waveguide, in which the waveguide mode is tightly confined between metal cladding placed immediately above and below the ~10 μm thick epitaxial active region. The overall result resembles a microstrip transmission line. MM waveguides tend to have the best high-temperature performance, mostly as a result of lower overall losses (both absorption and radiative) compared to the SP waveguide. Furthermore, the strong modal confinement of MM waveguides allows both the vertical and lateral dimensions to be made much smaller than the wavelength. This feature is unique for a new genre of lasers termed "photonic wire lasers", in which a large fraction of mode propagates outside of the solid core. This in turn reduces the total thermal dissipation and required cooling power, which was key to observation of the highest temperature cw operation (129 K) in a metal-metal waveguide (Wienold *et al.*, 2014). Furthermore, it is possible to mechanically perturb the portion of the mode outside the core using MEMS actuators, which has allowed broad single-mode tuning of up to 330 GHz (Qin *et al.*, 2011).

While metal-metal waveguides are preferred in terms of temperature performance, if a MM ridge waveguide is simply cleaved to form a Fabry-Pérot cavity, it performs poorly as an edge emitting laser. The cleaved facet radiates as a sub-wavelength sized aperture, which exhibits an extremely divergent beam with a poor radiation efficiency. Hence, an active area of research has emerged in the design of novel cavity types to allow high quality beams simultaneously with high output power.

A straightforward approach is to mount a silicon lens flush to the metal-metal waveguide facet, which helps to improve the beam quality and improve the impedance matching. Another class of approaches uses Bragg scattering from periodic structures to reshape the beam. Second-order distributed feedback (DFB) and 2D photonic crystal cavities have demonstrated surface emission; the beam is much improved since the waveguide surface, not the facet, is now the radiating aperture. One challenge that emerges is that the DFB laser prefers to lase in the mode with the lowest total losses, which usually is a weakly radiating (high-Q) band-edge mode with low output power. A variety of schemes are under investigation, including graded photonic heterostructures that force the laser to lase in the strongly radiating symmetric band-edge mode, and other structures (e.g. quasi-periodic crystals, dual slit gratings, and others) that break the lattice symmetry to increase radiative efficiency.

End-fire QC-lasers based upon 3rd-order DFBs or antenna-coupled DFB cavities are another attractive option; they can achieve very narrow far field beams even when the transverse waveguide cross section is sub-wavelength (Amanti *et al.*, 2009). The beam is formed by a linear phased array of scatters along the length of the cavity; the beam divergence scales inversely with square root of the cavity length for a perfectly phase-matched 3rd-order DFB laser. Hence, this allows narrow photonic wire cavities to be used, which further keeps the power dissipation low for good cw operation. Slope efficiencies can be made large by including antenna-like structures into the cavity. These approaches are particularly effective for milliwatt-scale power output.

Still another class of approaches involves the phase locking of multiple smaller emitting elements to achieve high quality beams and to scale up the power by power combining. While arrays of 2nd order DFBs have been demonstrated, it is challenging to phase lock more than a few elements. Two new approaches address this issue. One is to use radiative coupling to couple large arrays of sub-wavelength sized QC-laser cavities – for appropriate lattice spacings the individual cavities will prefer to lase in an in-phase collective supermode that provides a directive high quality beam with high slope efficiency (Kao *et al.*, 2016). If this array is biased slightly below threshold, it can be used as a reflective THz amplifier. The other approach is similar, but deliberately uses arrays of sub-wavelength cavities with low-quality factor (so they do not self-oscillate) to form a reflective amplifying "metasurface". When this metasurface is placed into an external cavity, these emitters lock to the cavity mode (Xu *et al.*, 2015). Such a device, known as a metasurface vertical-emitting-cavity surface-emitting-laser (VECSEL), not only allows scalable power with a high-quality beam, but detailed control over the phase, spectral, and polarization response of the metasurface.

## THz QC-Laser Frequency Combs

A rapidly evolving area of current research is the development of broadband, multi-mode THz QC-lasers that operate as frequency combs (Burghoff *et al.*, 2014). QC-lasers can be designed to exhibit gain over very large fractional gain bandwidths. This feature emerges naturally because certain designs of active region exhibit emission from multiple broadened transitions; furthermore, the active region can be made deliberately inhomogeneous by sandwiching multiple stacks, each intended to emit at different wavelengths (Rösch *et al.*, 2015). If the intracavity dispersion is properly managed (so that each longitudinal mode sees the same round trip time), then the multiple modes will interact via four-wave-mixing to establish a phase coherent comb. This is a different mechanism than the traditional method of comb generation based upon ultrafast mode-locked lasers - instead of a circulating intracavity pulse, the intensity inside the laser cavity is much closer to a constant value.

Perhaps the largest application is rapid, high-precision dual-comb spectroscopy, in which two combs (signal and local oscillator) with slightly detuned comb tooth spacings are mixed. This technique effectively mimics the functionality of Fourier-Transform Spectroscopy, but without the need for a mechanically moving mirror. The best reported comb bandwidths are approximately 1 THz, which still falls short of the octave spanning bandwidth needed to allow f-2f self-stabilization of the comb. For this reason, a major focus of current research is the effort to increase the comb bandwidth, by engineering both the active region and the cavity dispersion, in order to increase the gain bandwidth while simultaneously managing dispersion.

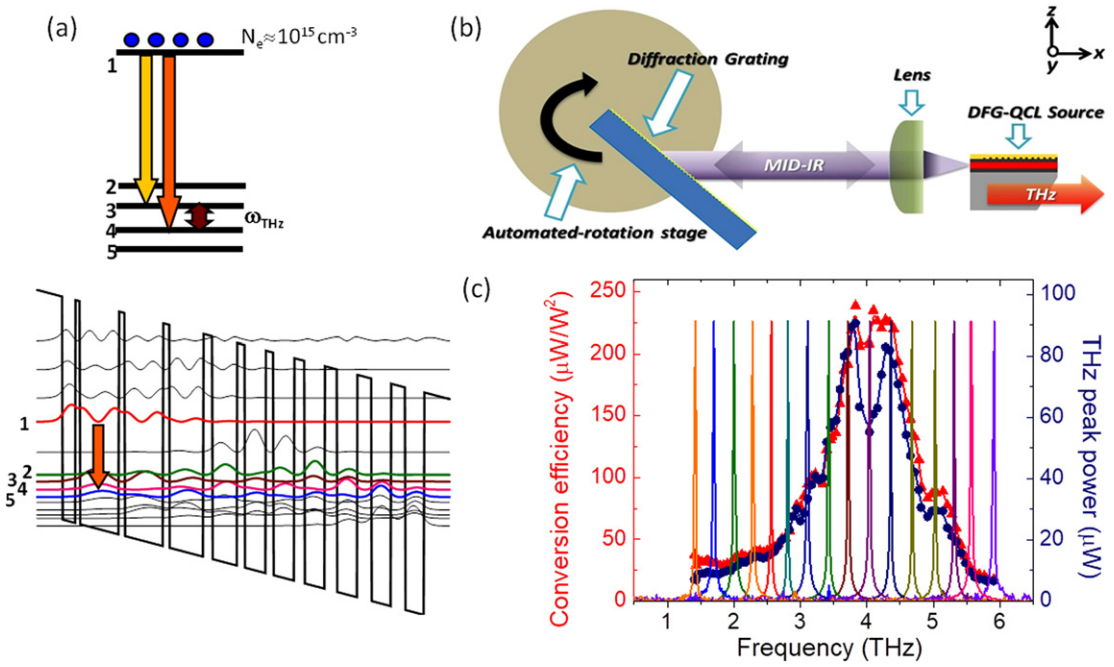


**Fig. 6** (a) Schematic of mid-IR QC-laser active region band diagram, indicating the levels primarily involved with the DFG process. (b) Schematic of external cavity setup for tunable THz DFG. (c) Spectra of THz DFG over tuning range. Figure adapted from Vijayraghavan, K., Jiang, Y., Jang, M. *et al.*, 2013. Broadly tunable terahertz generation in mid-infrared quantum cascade lasers. Nat. Commun. 4, 2021.

## Nonlinear Generation of THz Radiation in Mid-IR QC-Lasers

There exists a separate approach for generating THz radiation in QC-lasers that uses nonlinear downconversion from shorter wavelengths rather than direct lasing. Specifically, room-temperature THz radiation has been generated using intracavity difference frequency generation (DFG) within mid-infrared QC-lasers lasing at two wavelengths (Belkin *et al.*, 2007). Generation of THz radiation in nonlinear crystals via downconversion has a long history - however usually the limited strength of the available $\chi^{(2)}$ nonlinearity has required large laser intensities; as a result these techniques have required high power pulsed lasers (both Q-switched and mode-locked) in the visible and near-IR.

Mid-IR QC-lasers with wavelengths near 10 μm are more attractive, since the smaller pump photon energy results in an improved Manley-Rowe ratio, and the lasers themselves are physically smaller. Furthermore, the quantum-cascade laser material itself can be engineered to possess an extremely large resonant $\chi^{(2)}$ nonlinearity based upon the mid-IR intersubband transitions (**Fig. 6**). Ordinarily, resonant nonlinearities are accompanied by large linear absorption losses, but because this nonlinearity is associated with the same intersubband transitions that produce the mid-IR laser gain, the resonant absorption is avoided. This allows efficient mixing to take place within the laser cavity, where the circulating intensities are high. This approach leverages the greater technological maturity of mid-IR lasers in the 4–10 μm range, where room-temperature continuous-wave operation is possible with hundreds of mW or more.

While the initial demonstrations of THz DFG had very low conversion efficiency and sub-microwatt pulsed powers, significant advances have taken place recently. Currently, the highest reported THz power levels at room-temperature are 1.9 mW of peak power in pulsed mode, and 14 $\mu$W of power in cw mode (Lu and Razeghi, 2016). These sources are particularly promising for applications which require broad tunability, since only modest tuning of one of the mid-IR modes translates to large tuning of the THz beat note. For example, tuning of a single mode from 1.7–5.3 THz was shown in (Vijayraghavan *et al.*, 2013). Work is underway to further increase the nonlinear conversion efficiency, improve the efficiency of out-coupling the THz radiation from the cavity, as well as the increase the range and ease of tunability.

*See also*: Broadband Terahertz Sources. THz Molecular Spectroscopy

## References

Amanti, M.I., Fischer, M., Scalari, G., Beck, M., Faist, J., 2009. Low-divergence single-mode terahertz quantum cascade laser. Nature Photon. 3, 586–590.
Belkin, M.A., Capasso, F., Belyanin, A., *et al.*, 2007. Terahertz quantum-cascade-laser source based on intracavity difference-frequency generation. Nature Photon. 1, 288–292.

Blom, A., Odnoblyudov, M.A., Cheng, H.H., Yassievich, I.N., Chao, K.A., 2001. Mechanism of terahertz lasing in SiGe/Si quantum wells. Appl. Phys. Lett. 79, 713.
Bründermann, E., Chamberlin, D.R., Haller, E.E., 2000. High duty cycle and continuous terahertz emission from germanium. Appl. Phys. Lett. 76, 2991.
Burghoff, D., Kao, T.-Y., Han, N., *et al.*, 2014. Terahertz laser frequency combs. Nat. Photon. 8, 462–467.
Chang, T.Y., Bridges, T.J., 1970. Laser action at 452, 496, and 541 μm in optically pumped $CH_3F$. Opt. Commun. 9, 423–426.
Crocker, A., Gebbie, H.A., Kimmitt, M.F., Mathias, L.E.S., 1964. Stimulated emission in the far infra-red. Nature 201, 250–251.
Dodel, G., 1999. On the history of far-infrared (FIR) gas lasers: thirty-five years of research and application. Infrared Phys. Technol. 40, 127–139.
Farhoomand, J., Blake, G.A., Frerking, M.A., Pickett, H.M., 1985. Generation of tunable sidebands in the far-infrared region. Proc. SPIE 598, 84–87.
Golka, S., Pflügl, C., Schrenk, W., Strasser, G., 1991. Special issue – Far-infrared semiconductor lasers. Opt. Quantum Electron. 23, S111.
Gousev, Y.P., Altukhov, I.V., Korolev, K.A., *et al.*, 1999. Widely tunable continuous-wave THz laser. Appl. Phys. Lett. 75, 757.
Hovenier, J.N., Diez, M.C., Klassen, T.O., *et al.*, 2000. The p-Ge terahertz laser propeties under pulsed- and mode-locked operation. IEEE Trans. Microwave Theory Tech. 48, 670.
Hübers, H.-W., Pavlov, S.G., Shastin, V.N., 2005. Terahertz lasers based on germanium and silicon. Semicond. Sci. Technol. 20, S211–S221.
Inguscio, M., Moruzzi, G., Evenson, K.M., Jennings, D.A., 1986. A review of frequency measurements of optically pumped lasers from 0.1 to 8 THz. J. Appl. Phys. 60, R161.
Jacobsson, S., 1989. Optically pumped far infrared lasers. Infrared Phys 29, 853–874.
Kagan, M.S., Altukhov, I.V., Sinis, V.P., *et al.*, 2000. Terahertz emission of SiGe/Si quantum wells. Thin Solid Films 380, 237.
Kao, T.-Y., Reno, J.L., Hu, Q., 2016. Phase-locked laser arrays through global antenna mutual coupling. Nat. Photon.
Köhler, R., Tredicucci, A., Beltram, F., *et al.*, 2002. Terahertz semiconductor-heterostructure laser. Nature 417, 156.
Kumar, S., 2011. Recent progress in terahertz quantum cascade lasers. IEEE J. Sel. Top. Quantum Electron. 17, 38–47.
Lu, Q., Razeghi, M., 2016. Recent advances in room temperature, high-power terahertz quantum cascade laser sources based on difference-frequency generation. Photonics 3, 42.
Mueller, E.R., Henschke, R., William, E., *et al.*, 2007. Terahertz local oscillator for the Microwave Limb Sounder on the Aura satellite. Appl. Opt. 46, 4907–4915.
Pavlov, S.G., Zhukavin, R.K., Shastin, V.N., Hubers, H.-W., 2013. The physical principles of terahertz silicon lasers based on intracenter transitions. Phys. Status Solidi B 250, 9–36.
Qin, Q., Reno, J.L., Hu, Q., 2011. MEMS-based tunable terahertz wire-laser over 330GHz. Opt. Lett. 36, 692–694.
Rochat, M., Ajili, L., Willenberg, H., *et al.*, 2002. Low-threshold terahertz quantum-cascade lasers. Appl. Phys. Lett. 81, 1381.
Rösch, M., Scalari, G., Beck, M., Faist, J., 2015. Octave-spanning semiconductor laser. Nat. Photon. 9, 42–47.
Vijayraghavan, K., Jiang, Y., Jang, M., *et al.*, 2013. Broadly tunable terahertz generation in mid-infrared quantum cascade lasers. Nat. Commun. 4, 2021.
Vitiello, M.S., Scalari, G., Williams, B.S., Denatale, P., 2015. Quantum cascade lasers: 20 years of challenges. Opt. Express 23, 5167–5182.
Wade, A., Federov, G., Smirnov, D., *et al.*, 2009. Magnetic-field-assisted terahertz quantum cascade laser operating up to 225 K. Nat. Photon. 3, 41–45.
Wienold, M., Röben, B., Schrottke, L., *et al.*, 2014. High-temperature, continuous-wave operation of terahertz quantum-cascade lasers with metal-metal waveguides and third-order distributed feedback. Opt. Express 22, 3334–3348.
Williams, B.S., 2007. Terahertz quantum cascade lasers. Nat. Photon. 1, 517–524.
Williams, B.S., Callebaut, H., Kumar, S., Hu, Q., Reno, J.L., 2003. 3.4-THz quantum cascade laser based on longitudinal-optical-phonon scattering for depopulation. Appl. Phys. Lett. 82, 1015.
Xu, L., Curwen, C.A., Hon, P.W.C., *et al.*, 2015. Metasurface external cavity laser. Appl. Phys. Lett. 107, 221105.